

The inner structure of haloes in Cold+Warm dark matter models

Andrea V. Macciò^{1*}, Oleg Ruchayskiy², Alexey Boyarsky^{3,4}, Juan C. Muñoz-Cuartas⁵

¹ *Max-Planck-Institut für Astronomie, Königstuhl 17, 69117 Heidelberg, Germany.*

² *CERN Physics Department, Theory Division, CH-1211 Geneva 23, Switzerland*

³ *Instituut-Lorentz for Theoretical Physics, Universiteit Leiden, Niels Bohrweg 2, Leiden, The Netherlands*

⁴ *Bogolyubov Institute of Theoretical Physics, Kyiv, Ukraine*

⁵ *Leibniz-Institut für Astrophysik Potsdam, An der Sternwarte 16, 14482 Potsdam, Germany*

Accepted XXXX, Received XXXX

ABSTRACT

We analyze the properties of dark matter halos in the cold-plus-warm dark matter cosmologies (CWDM). We study their dependence on the fraction and velocity dispersion of the warm particle, keeping the free-streaming scale fixed. To this end we consider three models with the same free-streaming: (1) a mixture of 90% of CDM and 10% of WDM with the mass 1 keV; (2) a mixture of 50% of CDM and 50% of WDM with the mass 5 keV; and (3) pure WDM with the mass 10 keV. “Warm” particles have rescaled Fermi-Dirac spectrum of primordial velocities (as non-resonantly produced sterile neutrinos would have). We compare the properties of halos among these models and with a Λ CDM with the same cosmological parameters. We demonstrate, that although these models have the same free-streaming length and the suppression of matter spectra are similar at scales probed by the Lyman- α forest (comoving wave-numbers $k < 3 - 5$ h/Mpc), the resulting properties of halos with masses below $\sim 10^{11} M_{\odot}$ are different due to the different behaviour of matter power spectra at smaller scales. In particular, we find that while the number of galaxies remains the same as in Λ CDM case, their density profiles become much less concentrated, and hence in better agreement with current observational constraints. Our results imply that a single parameter (e.g. free streaming length) description of these models is not enough to fully capture their effects on the structure formation process.

Key words:

1 INTRODUCTION

It is usually said that cosmological data favour *Cold* Dark Matter. The cosmological “concordance model” is therefore often called Λ CDM. However, a more precise statement should be that *hot* dark matter particles (i.e. the particles that became non-relativistic only around recombination time, such as e.g. the ordinary neutrinos) are ruled out (Davis et al. 1985). The difference between cold and *warm* DM particles (the former being always non-relativistic and the latter becoming non-relativistic deeply in the radiation-dominated epoch) would show up at approximately galactic scales and it is only recently that such small scale effects are starting to be resolvable both theoretically (see e.g. Macciò & Fontanot 2010; Polisensky & Ricotti 2011; Markovic et al. 2011; Semboloni et al. 2011; van Daalen et al. 2011;

Lovell et al. 2012; Viel et al. 2011; Smith & Markovic 2011; Schneider et al. 2012; Dunstan et al. 2011, and refs. therein) and experimentally (see e.g. Viel et al. 2005, 2006; Seljak et al. 2006; Viel et al. 2008; Boyarsky et al. 2009a; Tikhonov et al. 2009; Zavala et al. 2009; Song & Lee 2009; Papastergis et al. 2011). Warm dark matter N-body simulations require significantly larger number of particles to resolve the same scales as compared with the CDM case (see e.g. Wang & White 2007; Lovell et al. 2012). Additionally, at sub-Mpc scales baryonic physics can hide (or mimic) the WDM suppression of power (see e.g. (Benson et al. 2002; Bullock et al. 2000; Semboloni et al. 2011), which makes the analysis of small-scale data challenging.

The tiny (from the cosmological point of view) difference between cold and warm dark matter is however of crucial importance for particle physics, as it means a huge difference in the properties of corresponding particles and may eventually provide a clue on the structure of a fundamental theory of particles and interactions.

* email: maccio@mpia.de

Historically the first WDM models were *thermal relics* – particles that were in equilibrium in the early Universe and froze-out, being relativistic (Colin et al. 2000; Bode et al. 2001). Such particles had thermal primordial velocity spectrum and strong cutoff-like suppression of the power spectra (Bode et al. 2001; Viel et al. 2005; Boyarsky et al. 2009a) at scales below few Mpc. Such models are characterized by only one scale — position of the cutoff in the power spectrum, related to their free-streaming horizon. One possible tool to probe the growth of structures of (sub)Mpc scales is the Lyman- α forest method – studies of statistics of absorption features in the spectra of distant quasars. The Lyman- α forest data (Hansen et al. 2002; Viel et al. 2005, 2006; Seljak et al. 2006; Viel et al. 2008; Boyarsky et al. 2009a) puts such strong constraints at their free-streaming length that “thermal relics” WDM models, compatible with Lyman- α bounds, produce essentially no observable changes in the Galactic structures (c.f. Strigari et al. 2006; Colin et al. 2008; Boyarsky et al. 2009a; de Naray et al. 2009; Schneider et al. 2012).

However, particle physics motivated WDM candidates can be produced in the early Universe in non-thermal ways, may have significant non-zero primordial velocities in the radiation-dominated epoch and non-equilibrium velocity spectra (for review see e.g. Boyarsky et al. 2009b,c; Taoso et al. 2008; Feng 2010). In many models (e.g. sterile neutrinos, gravitino, axino) the same DM particles can be produced via two co-existing mechanisms and therefore generically primordial velocity spectra have “colder” and “warmer” components. Such models can be called *mixed* or “cold plus warm” dark matter models (**CWDM**) (Boyarsky et al. 2009a, see also Palazzo et al. 2007). Qualitatively, structures form in these models in a bottom-up fashion (similar to CDM). The way the scales are suppressed in CWDM models is more complicated (and in general less severe for the same masses of WDM particles), as comparable with pure warm DM models. The first results of Lovell et al. (2012) demonstrate that the resonantly produced sterile neutrino DM models, compatible with the Lyman- α bounds of Boyarsky et al. (2009b), do change the number of substructure of a Galaxy-size halo and their properties. The discrepancy between the number of observed substructures with small masses and those predicted by Λ CDM models (first pointed out in Klypin et al. 1999; Moore et al. 1999) can simply mean that these substructures did not confine gas and are therefore completely dark (see e.g. Bullock et al. 2000; Benson et al. 2002; Somerville 2002; Macciò et al. 2010). This is not true for larger objects. In particular, CDM numerical simulations invariably predict several satellites “too big” to be masked by galaxy formation processes, in contradiction with observations (Boylan-Kolchin et al. 2011). Sterile neutrino DM of the minimal neutrino extension of the Standard Model (the ν MSSM) Asaka & Shaposhnikov (2005); Boyarsky et al. (2009c), with its non-trivial velocity dispersion, turns out to be “warm enough” to amend these issues (Lovell et al. 2012) and “cold enough” to be in agreement with Lyman- α bounds (Boyarsky et al. 2009b).

In this paper we study the structures of halos in the CWDM models. To this end we pick two CWDM models, compatible with the Lyman- α data of Boyarsky et al. (2009a) and having the same free-streaming of the WDM

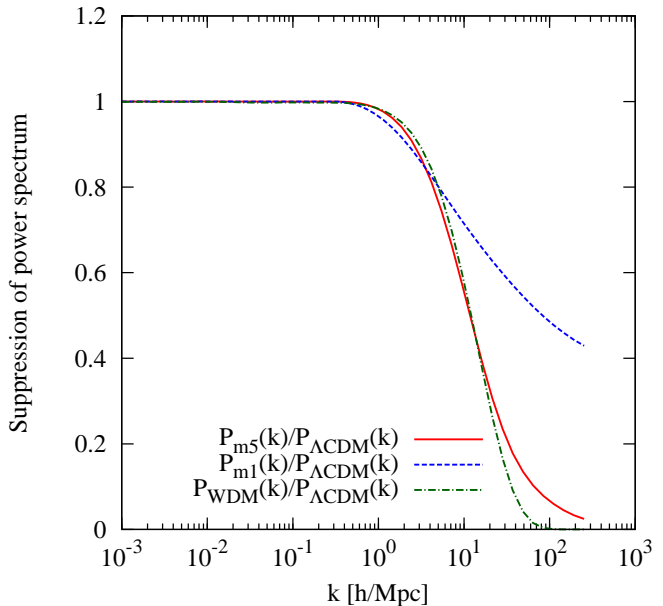


Figure 1. Ratio of the power spectra of the three models used in this work to that of Λ CDM (for the same values of cosmological parameters). The blue short-dashed curve is a mixture of 90% of cold dark matter and 10% warm dark matter with rescaled Fermi-Dirac spectrum and mass $m_{\text{WDM}} = 1$ keV, (model **m1**); the red solid line is a mixture 50% of cold and warm particles with the mass $m_{\text{WDM}} = 5$ keV (model **m5**) and the green dashed-dotted line (model **wdm**) is a 100% WDM model with the mass of DM particle $m_{\text{WDM}} = 10$ keV. All three models are compatible with the Lyman- α analysis of Boyarsky et al. (2009a).

particles. We demonstrate that the properties of halos differ in these models (and differ from both pure CDM and pure WDM model with the same free-streaming), meaning that they are not determined by the free-streaming alone.

The paper is organized as follows. We discuss the choice of parameters of our DM models and initial conditions for simulations in Section 2. The suite of simulations is discussed in Sec. 3 and the main results in Section 4. We discuss our results in Section 5.

2 MODEL SELECTION AND INITIAL CONDITIONS

For our simulations we selected two CWDM, one WDM and one reference Λ CDM model. Our first CWDM model (model **m1** in what follows) is a mixture of 90% of cold dark matter and 10% of warm dark matter with the mass $m_{\text{wdm}} = 1$ keV, while the second is a 50% cold and warm mixture with the mass $m_{\text{wdm}} = 5$ keV (model **m5** hereafter). The WDM model has $m_{\text{wdm}} = 10$ keV. In all cases the WDM components have the rescaled Fermi-Dirac spectrum of primordial velocities

$$f(v) = \frac{\chi}{\exp\left(\frac{m_{\text{wdm}} v}{T_\nu(z)}\right) + 1} \quad (1)$$

where m_{wdm} is the WDM mass, $T_\nu(z)$ is the temperature of cosmic neutrino background, evolving with redshift as $T_\nu(z) = T_{\nu 0}(1+z)$, $T_{\nu 0} = 1.9$ K, and the constant χ is

determined by the requirement to provide a given fraction, F_{wdm} , of the total dark matter density:

$$m_{\text{wdm}}^4 \int \frac{d^3v}{(2\pi)^3} f(v) = F_{\text{wdm}} \rho_{\text{DM}} \quad (2)$$

(in the units where $c = \hbar = k_B = 1$). Non-resonantly produced sterile neutrinos would have such a phase-space distribution (1) (Dodelson & Widrow 1994; Dolgov & Hansen 2002). One can relate the parameters of such WDM models and those of “thermal relics” (Bode et al. 2001), using e.g. formulas in Viel et al. (2005). In order to investigate the dependence of the properties of the cosmologies on parameters other than free-streaming (i.e. WDM mass and F_{wdm} component), we have chosen the models in such a way that their *free-streaming horizon is the same*. Both models are compatible with the CWDM Lyman- α analysis of Boyarsky et al. (2009a).

We computed the *linear* power spectrum at redshift $z_{\text{ini}} \sim 30$ of matter density perturbations $P_{\text{ini}}(k, z_{\text{ini}})$ for these models. The standard software (i.e. CAMB, Lewis et al. 2000) is not immediately appropriate for this purpose, as it only treats massive neutrinos with a Fermi-Dirac primordial distribution. To adapt it to the problem at hand, we modified CAMB so that it could take arbitrary spectra as input data files. We analyzed the spacing in momentum space needed in order to obtain precise enough results, and implemented explicit computations of distribution momenta in CAMB. We cross-checked our results by modifying another linear Boltzmann solver – CMBFAST (Seljak & Zaldarriaga 1996), implementing a treatment of massive neutrinos with arbitrary *analytic* distribution function and with the CLASS code (Lesgourgues & Tram 2011) where such an option is realized.

Figure 1 shows the ratio of the power spectrum in our CWDM models with respect to the Λ CDM model with the same cosmological parameters. The effect of the free-streaming is clearly visible on scales smaller than $k \approx 1$ h/Mpc. It is important to notice that although the two models formally have the same free-streaming length, since the product of the WDM mass and its abundance is constant, the suppression of power on small scales is different in the two models and larger for the **m5** model, due to its more abundant warm dark matter component.

Based on the linear power spectrum $P_{\text{ini}}(k, z_{\text{ini}})$ the initial conditions for N-body simulations are generated with a modified version of the GRAFIC2 package (Bertschinger 2001). In this modified version the transfer function at the starting redshift is given as an external input. The starting redshifts z_i are set to the time when the standard deviation of the smallest density fluctuations resolved within the simulation box reaches 0.15 (the smallest scale resolved within the initial conditions is defined as twice the intra-particle distance). We used the best-fit cosmological parameters from Boyarsky et al. (2009a), comparable with WMAP5 results (Komatsu et al. 2009). Namely: $\Omega_m = 0.253$, $\Omega_\Lambda = 0.747$, $n = 0.973$, $h = 0.72$, and $\sigma_8 = 0.8$.

In our small box simulations ($L = 20 \text{ h}^{-1} \text{ Mpc}$) we also include the effect of a non zero primordial velocity dispersion for WDM particles. The streaming velocities were generated using the corresponding expression for the average primordial velocity $\langle v(z) \rangle$ given e.g. in Section 4 in Boyarsky et al. (2009a):

Name	Box size [$h^{-1} \text{ Mpc}$]	N	part. mass [$h^{-1} M_\odot$]	force soft. [$h^{-1} \text{ kpc}$]
Λ CDM-20	20	350^3	1.31e7	1.42
Λ CDM-45	45	350^3	1.49e8	3.21
Λ CDM-90	90	400^3	7.99e8	5.62
Λ CDM-180	180	400^3	6.39e9	11.25
WDM-20	20	350^3	1.31e7	1.42
WDM-45	45	350^3	1.49e8	3.21
m1-20vel	20	350^3	1.31e7	1.42
m1-20	20	350^3	1.31e7	1.42
m1-45	45	350^3	1.49e8	3.21
m1-90	90	400^3	7.99e8	5.62
m1-180	180	400^3	6.39e9	11.25
m5-20vel	20	350^3	1.31e7	1.42
m5-20	20	350^3	1.31e7	1.42
m5-45	45	350^3	1.49e8	3.21
m5-90	90	400^3	7.99e8	5.62
m5-180	180	400^3	6.39e9	11.25

Table 1. N-body simulation parameters

$$\langle v(z) \rangle = F_{\text{wdm}} \frac{3.151 T_\nu(z)}{m_{\text{wdm}}} \quad (3)$$

or numerically:

$$\langle v(z) \rangle = 15.7 \times F_{\text{wdm}} \left(\frac{1+z}{100} \right) \left(\frac{1 \text{ keV}}{m_{\text{wdm}}} \right) \text{ km.s}^{-1}. \quad (4)$$

where z is the redshift of the beginning of simulation, m_{wdm} is the mass of the WDM particle. We had kept the amplitude of primordial velocity constant and equal to (3) and randomly chosen the direction of velocities of the particles to add them to the Zel’dovich velocities, generated with the GRAFIC2 package.

3 NUMERICAL SIMULATIONS

All simulations have been performed with PKDGRAV, a tree code written by Joachim Stadel and Thomas Quinn (Stadel 2001). The code uses spline kernel softening, for which the forces become completely Newtonian at 2 softening lengths. Individual time steps for each particle are chosen proportional to the square root of the softening length, ϵ , over the acceleration, a : $\Delta t_i = \eta \sqrt{\epsilon/a_i}$. Throughout, we set $\eta = 0.2$, and we keep the value of the softening length constant in comoving coordinates during each run. The physical values of ϵ at $z = 0$ are listed in Table 1. Forces are computed using terms up to hexadecapole order and a node-opening angle θ which we change from 0.55 initially to 0.7 at $z = 2$. This allows a higher force accuracy when the mass distribution is nearly smooth and the relative force errors can be large.

Table 1 lists all of the simulations used in this work. We have run simulations for several different box sizes, which allows us to probe halo masses covering the entire range $10^{10} h^{-1} M_\odot \leq M \leq 10^{14} h^{-1} M_\odot$. For the small box simulations ($L = 20 \text{ Mpc/h}$) we have, for each CWDM model, two different runs, with and without thermal velocities.

Fig. 2 shows the halo mass function for the **m5** model at $z = 0$. Only haloes with viral masses larger than $2 \times 10^{10} h^{-1} M_\odot$ are shown, and different symbols (and colors) refer to different box size simulations. The green line is

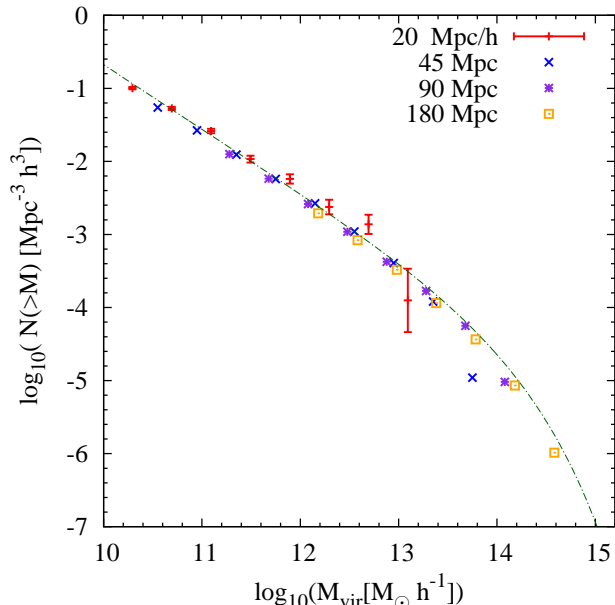


Figure 2. Halo mass function for all three models at $z = 0$ follow predictions of Λ CDM with the same cosmological parameters (green dashed line is the Warren et al. (2006) predictions for Λ CDM). Shown are the points for **m5** model, the other two models (**m1** and WDM) give very similar results and are not shown.

the Warren et al. (2006) prediction for a pure Λ CDM model with the same cosmological parameters as our CWDM models.

The Warren et al. (2006) prediction is a good representation of our data at high and low masses. The **m1** and WDM models present similar behaviours as the **m5** one.

3.1 Halo parameters

In all of the simulations, dark matter haloes are identified using a spherical overdensity (SO) algorithm. We use a time varying virial density contrast determined using the fitting formula presented in Mainini et al. (2003). We include in the halo catalog all the haloes with more than 500 particles (see Macciò et al. (2008) for further details on our halo finding algorithm). For each SO halo in our sample we determine a set of parameters, including the virial mass and radius, the concentration parameter, the angular momentum, the spin parameter and axis ratios (shape). Below we briefly describe how these parameters are defined and determined. A more detailed discussion can be found in Macciò et al. (2007, 2008). Finally following Macciò et al. (2007), we split our halo sample into unrelaxed and relaxed haloes. In the rest of the paper we will only discuss the properties of relaxed haloes.

3.1.1 Concentration parameter

To compute the concentration of a halo we first determine its density profile. The halo centre is defined as the location of the most bound halo particle, and we compute the density (ρ_i) in 50 spherical shells, spaced equally in logarithmic radius. Errors on the density are computed from the Pois-

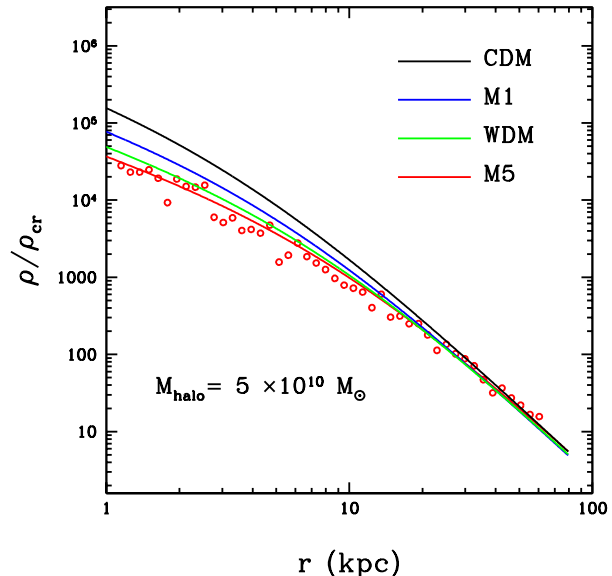


Figure 3. Density profiles for CWDM and WDM models. The plot shows the change in the inner slope of the halo density profile for one of the haloes in the simulation with the box size $L = 20$ Mpc/h (as compared to the CDM – black line). Points and red line (the NFW fit) are for the **m5** model. For **m1** and WDM models we show only the NFW fit (to make the plot less crowded). Black line shows the predicted profile for Λ CDM using the fitting formula from Muñoz-Cuartas et al. (2011).

son noise due to the finite number of particles in each mass shell. The resulting density profile is fit with a NFW profile (Navarro et al. 1997)¹:

$$\frac{\rho(r)}{\rho_c} = \frac{\delta_c}{(r/r_s)(1 + r/r_s)^2}, \quad (5)$$

During the fitting procedure we treat both r_s and δ_c as free parameters. Their values, and associated uncertainties, are obtained via a χ^2 minimization procedure using the Levenberg & Marquardt method. We define the r.m.s. of the fit as:

$$\rho_{\text{rms}} = \frac{1}{N} \sum_i^N (\ln \rho_i - \ln \rho_m)^2 \quad (6)$$

where ρ_m is the fitted NFW density distribution. Finally, we define the concentration of the halo, $c_{\text{vir}} \equiv r_{\text{vir}}/r_s$, using the virial radius obtained from the SO algorithm, and we define the error on $\log c$ as $(\sigma_{r_s}/r_s)/\ln(10)$, where σ_{r_s} is the fitting uncertainty on r_s .

3.1.2 Shape parameter

Determining the shape of a three-dimensional distribution of particles is a non-trivial task (e.g., Jing & Suto 2002).

¹ In this paper we do not resolve (due to resolution) and do not discuss the inner slope of DM density profiles, as for example in Macciò et al. (2012b). Therefore, possible deviations from the NFW profile due to WDM effects, even appearance of a core, are not considered.

Name	$z = 0$	$z = 0.5$	$z = 1$
$a(z)$	-0.0973	-0.0828	-0.0684
$b(z)$	2.157	1.845	1.578
$\alpha(z)$	-4.78e-6	-5.3095e-6	-4.6561e-6
$\beta(z)$	0.766	0.729	0.681

Table 2. Fitting parameter for the concentration and shape mass dependence

Following Allgood et al. (2006), we determine the shapes of our haloes starting from the inertia tensor. As a first step, we compute the halo’s 3×3 inertia tensor using all the particles within the virial radius. Next, we diagonalize the inertia tensor and rotate the particle distribution according to the eigenvectors. In this new frame (in which the moment of inertia tensor is diagonal) the ratios $s = a_3/a_1$ and $p = a_2/a_1$ (where $a_1 \geq a_2 \geq a_3$) are given by:

$$s \equiv \frac{a_3}{a_1} = \sqrt{\frac{\sum m_i z_i^2}{\sum m_i x_i^2}} \quad p \equiv \frac{a_2}{a_1} = \sqrt{\frac{\sum m_i z_i^2}{\sum m_i y_i^2}}. \quad (7)$$

Next we again compute the inertia tensor, but this time only using the particles inside the ellipsoid defined by a_1 , a_2 , and a_3 . When deforming the ellipsoidal volume of the halo, we keep the longest axis (a_1) equal to the original radius of the spherical volume (r_{vir}). We iterate this procedure until we converge to a stable set of axis ratios.

4 THE CONCENTRATION MASS RELATION

In Figure 4, we show the concentration mass relation for relaxed haloes in the Λ CDM model. In our mass range the $c_{\text{vir}} - M_{\text{vir}}$ relation is well fitted by a single power law at all redshifts, in agreement with several previous results (e.g. Klypin et al. (2011), and references therein). The best fitting power law can be written as:

$$\log(c) = a(z) \log(M_{\text{vir}}/[h^{-1} M_{\odot}]) + b(z). \quad (8)$$

The fitting parameter $a(z)$ and $b(z)$ are function of redshifts and are reported in table 2. These parameters are very not far from the ones suggested in Muñoz-Cuartas et al. (2011). From now on we will use these linear fits to compare (C)WDM models and the standard Λ CDM one.

Figure 5 (right) shows the mass and redshift dependence of the concentration parameter for the **m5** model. Results for $z = 0$, $z = 0.5$ and $z = 1$ are shown from top to bottom. The error-bars on the points show the error in the mean concentration value (while the scatter is of the order of 0.3 dex independently on the mass scale) The three lines are the fits to the Λ CDM results from figure 4.

At high masses the CWDM models basically agree with the pure cold dark matter predictions. The situation is different for masses below $10^{12} h^{-1} M_{\odot}$, where the CWDM model predicts lower concentrations with respect to the Λ CDM. For our lowest mass bin ($M \approx 10^{10} h^{-1} M_{\odot}$) the concentration is lower by 40% and there is a clear indication of flattening of the concentration mass relation, with an almost flat relation for $\log(M) < 10.5$. This flat tail of the cM relation at low masses is already in place at $z = 1$ and the

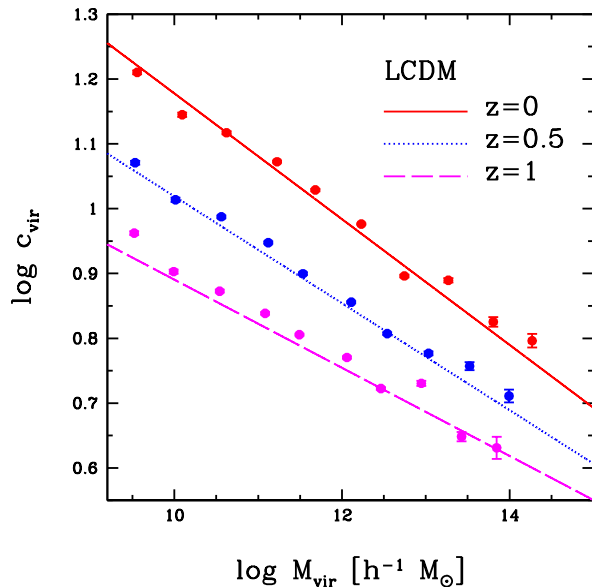


Figure 4. Mass and redshift dependence of the concentration parameter for the Λ CDM model with the same parameters as the mixed ones. Points with error-bars are simulation results, the straight lines are linear fits (in a log-log space) to the simulation results.

difference between CDM and CWDM appears to be redshift independent.

This results is not surprising. In CWDM models the formation of small haloes is delayed with respect to CDM due to the lack of power on small scales. The concentration parameter is related to the density of the universe at the time of the halo formation (Wechsler et al. 2002); since the density of the universe decreases with time, a later formation time implies a lower value for the concentration.

The **m1** model behaves similarly to **m5** (left panel of figure 5), showing a lower values for the concentration parameter (with respect to Λ CDM) at small masses. In this case the difference with Λ CDM is less pronounced and at the lowest mass scales ($M \approx 10^{11} h^{-1} M_{\odot}$) it is less than 15%.

The difference between **m1** and **m5** is a direct consequence of the different power spectrum at small scales. As shown in Figure 1 the **m5** model has less power at scales $k > 10$ h/Mpc, which correspond to mass scales of the order $8 \times 10^{10} h^{-1} M_{\odot}$. This lower power results in a later formation time for these halos and hence lower concentration. This is also confirmed by fig 6, where the concentration-mass relation for the WDM simulation is presented. Results for the pure WDM model are very similar to the **m5** model, confirming the relation between initial power spectrum (fig 1) and halo concentration.

The difference between the two CWDM models shows that even models with the same free-streaming length (as **m1** and **m5**) could lead to different halo internal structures. As a consequence the characterization of any models with a *warm* component only through its matter power spectrum suppression could lead to misleading results, since this single parameter is not capable to fully describe the effects of

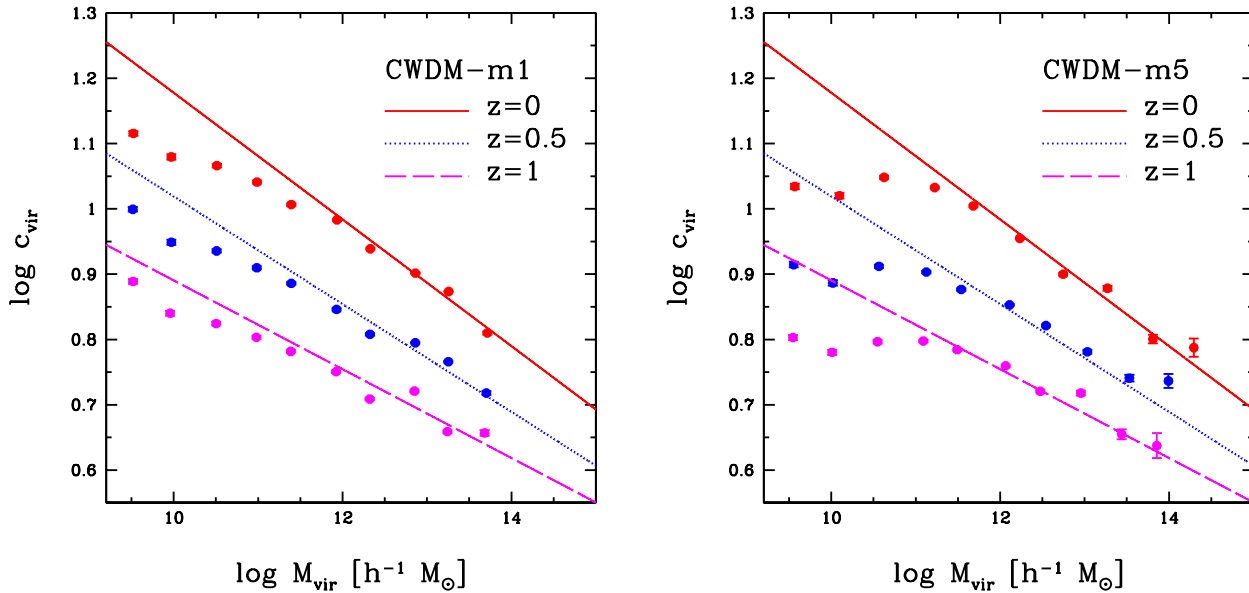


Figure 5. Mass and redshift dependence of the concentration parameter. Points with error-bars are CWDM simulation (**m1** and **m5** models at left and right panel correspondingly) results, the three straight lines are the fits to the CDM results from figure 4. From top to bottom: $z = 0$, $z = 0.5$, $z = 1$. One sees that **m1** model is “colder” (closer to the CDM) than **m5** at all redshifts.

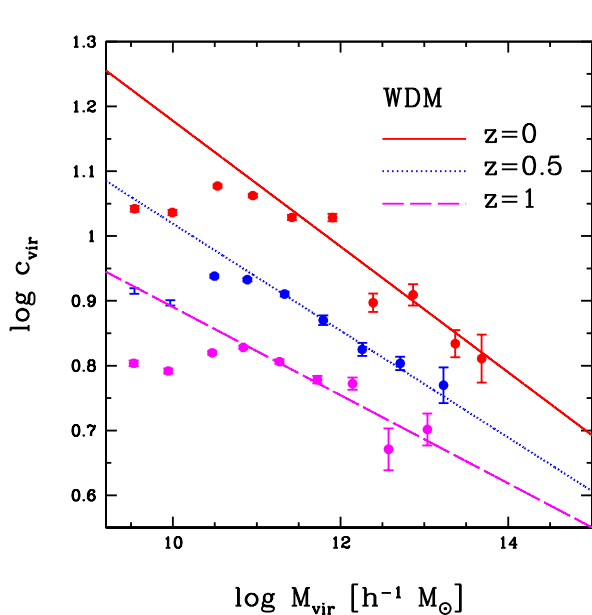


Figure 6. Same as fig. 5 for the WDM simulation. Notice the similarity with Fig. 5, right panel

a warm dark matter candidate on the structure formation process.

4.1 Effects of thermal velocities

For the small boxes (20 Mpc/h) we also run an additional simulation that included a thermal velocity component in the initial conditions. This thermal component is few percent

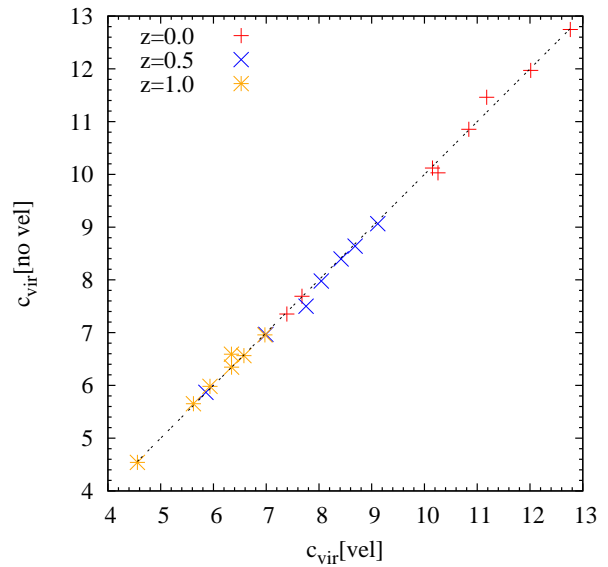


Figure 7. Effects of thermal velocities on the concentration parameter in the $20 h^{-1}$ Mpc box. Different symbols refer to different redshifts.

of the initial velocity due to the potential field (according to the Zel’dovich approximation), nevertheless it is important to test its effects (if any) on the halo internal structure.

Figure 7 shows the one-to-one comparison of the median c_{vir} at a given halo mass for the model **m1**, with and without primordial thermal velocities. As expected given the magnitude of the thermal velocity component, the effect is negligible. The model **m5** presents the same behaviour. The thermal velocity component will play a role on smaller scales

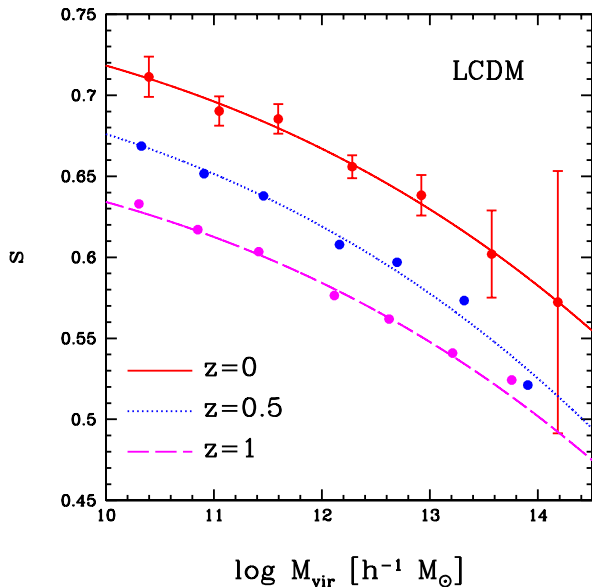


Figure 8. Mass and redshift dependence of the halo shape for the Λ CDM model with the same parameters as the mixed ones. Points with error-bars (shown only for the $z = 0$ case) are simulation results, lines are polynomial fits to Eq. (9).

(for example for Milky Way satellites) and we plan to address this issue in a forthcoming paper.

4.2 Effects on halo shape

There is a well known relation between halo shape and mass with low mass haloes being less triaxial (higher value for the s parameter) than high mass ones (Allgood et al. 2006; Macciò et al. 2008; Muñoz-Cuartas et al. 2011). This relation is usually explained by assuming that the halo “triaxiality” correlates with formation time, such that early halos have more time to virialize and hence reach a more equilibrated, less triaxial configuration. In this is the case we could possibly see a different trend between halo shape and mass in the CWDM simulation with respect to the Λ CDM.

Figure 8 shows the redshift and mass dependence of the shape parameter s for the Λ CDM model. In order to fit this relation we used the same equations as suggested by Muñoz-Cuartas et al. (2011):

$$s(z, M) = \alpha(z)(\log(M_{\text{vir}})/[h^{-1}M_{\odot}])^4 + \beta(z). \quad (9)$$

The values of the fit parameters ($\alpha(z), \beta(z)$) are listed in Table 2.

Figure 9 shows the redshift evolution of the halo shape, quantified via the minor to major axis ratio: $s \equiv a_3/a_1$, for the **m1** and **m5** models (left and right panels in Fig. 9 correspondingly).

In this case the CWDM models behaviour is very similar to Λ CDM and the two family models (Λ CDM and CWDM) seem to be consistent within the errors. Nevertheless there is a small hint for a lower values for the s parameter (hence a larger triaxiality) at the very low mass bins ($\approx 10^{10.3}h^{-1}M_{\odot}$), as expected due to the later formation times at these mass scales.

5 SUMMARY AND DISCUSSION

Interest in warm dark matter models has increased in the last years, mainly motivated by the possible need for cored (or very low concentration) dark matter halo density profiles for dwarf galaxies in the local group (see e.g. Walker & Penarrubia 2011; Amorisco & Evans 2011), or by solution of various CDM “over-abundance problems” (Klypin et al. 1999; Moore et al. 1999), see e.g. (Macciò & Fontanot 2010; Strigari et al. 2010; Boylan-Kolchin et al. 2011; Papastergis et al. 2011; Lovell et al. 2012).

While it is still under debate what is the effects of baryons on the dark matter distribution on such small scales (e.g. Pontzen & Governato 2012; Macciò et al. 2012a and references therein); it is worth studying through numerical simulations the effects of a warm component on the inner structure of DM haloes. It had been repeatedly argued that “pure warm” dark matter models (with a cutoff-like suppression of the matter power spectrum) could not be a solution to the core-cusp problem as the required free-streaming would be in a stark contradiction with Lyman- α bounds (see e.g. Strigari et al. 2006; de Naray et al. 2009).

In this paper we have performed the first N-body simulations for *cold plus warm* dark matter models (CWDM). In this class of models the dark matter particle candidate (e.g. sterile neutrinos, gravitino, axions) can be produced via two co-existing mechanisms and therefore the primordial spectrum is a superposition of a cold and a warm component, plus a complicated non-thermal velocity spectrum (e.g. Boyarsky et al. 2009b)

We have mainly focused our attention on the inner structure of dark matter haloes in CWDM models, and its evolution with redshift. We have adopted the commonly used *concentration* parameter (e.g. Macciò et al. 2008) to parameterize the modification in CWDM models with respect to the standard Cold Dark Matter (CDM) model.

We show that in our models the number of halos remains the same as in Λ CDM down to the smallest scales resolved in the simulations ($\sim 10^{10}M_{\odot}$). At the same time, keeping the free-streaming scale the same, the variation of WDM fraction is able to reduce the concentration parameter on mass scales as high as $M \approx 10^{12}h^{-1}M_{\odot}$, two/three order of magnitude above the free streaming mass of the model. On dwarf galaxies mass scale ($M \approx 10^{10}h^{-1}M_{\odot}$) the concentration parameter is almost half of the value predicted by Λ CDM and we see a clear sign of a strong flattening of the concentration mass relation. As a consequence we expect an even stronger concentration reduction on lower mass scales (below our resolution limits), mass scales directly explored by the Milky Way satellites. This decrease of the concentration of such large halos may explain why the “cuspy” matter distributions are not supported by observations of the rotation curves of spiral galaxies (see e.g. Salucci & Burkert 2000; Oh et al. 2008; Spano et al. 2008; de Naray et al. 2009), thus resolving one of the major challenges for the CDM cosmological model.

Another interesting result is the intrinsic difference in the concentration mass relation between the **m1** and **m5** models, that clearly shows that even models with the same free-streaming length could lead to different halo internal structures. As a consequence this calls for a detailed anal-

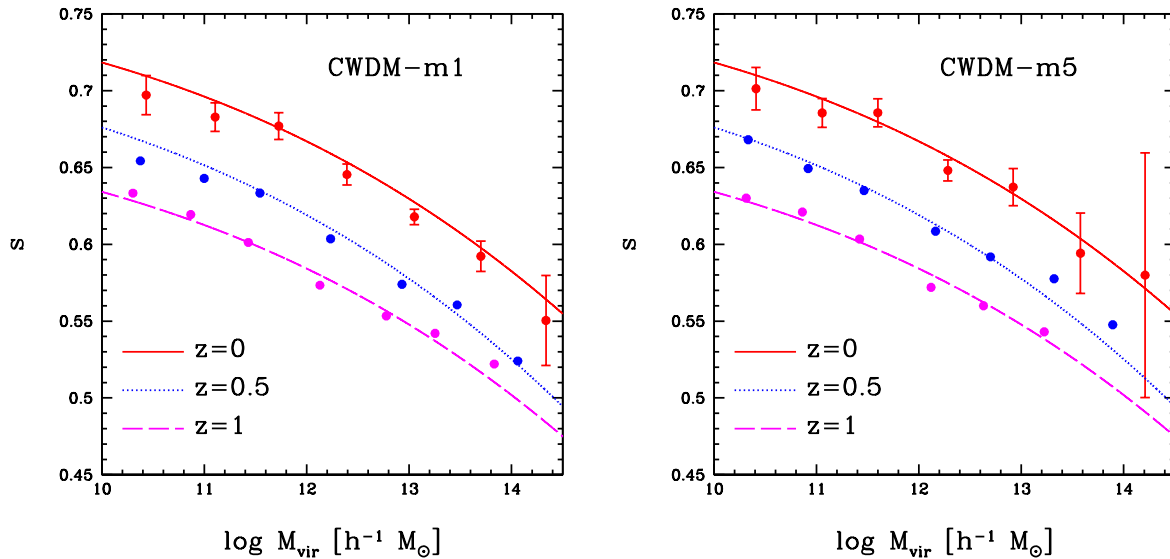


Figure 9. Mass and time evolution of the shape of dark matter haloes quantified via the $s \equiv a3/a1$ ratio. Lines are polynomial fits to Eq. (9) as in Fig. 8. Left panel – **m1** model, right panel – **m5** model

ysis of *any* model with a warm component, since a single parameter description through the free-streaming length is not capable to fully capture the effects on structure formation.

In Macciò et al. (2012b) it was shown that the primordial velocities required to produce the cores of observable sizes in pure WDM cosmologies are so large that too few galaxies would be formed. This is because in pure warm dark matter models the phase-space density, defining the size of the core and suppression in the halo number density are defined by the same parameter – the average velocity of particles. Our results show that in the CWDM models the presence of the second parameter, F_{wdm} , allows to control the “warmness” of dark matter, separating the scales of modification of the matter power spectrum (halo number density) and that of modification of the density profile (size of the core).

We stress that unlike the recent work of Macciò et al. (2012b) this effect is not related to the finite phase-space density (the phase-space density of particles in our simulations is the same as in pure CDM ones). We ascribe the lower concentration at small masses to a shift in the halo formation time, that results in a delayed formation for CWDM models with respect to CDM, as already found in previous studies (Eke et al. 2001; Lovell et al. 2012). This delayed formation time could also be responsible of the lower ratio between the halo minor and major axis (s parameter) that we saw at very low masses (even if the CWDM models are consistent with Λ CDM within the error-bars). We did not find any effect on the halo spin parameter distribution, which looks almost identical in all models.

We also tested the effect of explicitly including thermal velocities in the N-body initial conditions, We did not see any visible change in the concentration mass relation on the mass scales we are able to resolve. We plan to study in more details the importance of this thermal velocity component

in a forthcoming paper, by employing “zoomed” high resolution simulations of single dark matter haloes.

Along with the Lyman- α forest method, the weak lensing surveys can be used to probe further clustering properties of dark matter particles as sub-galactic scales, as the next generation of these surveys (such as e.g. KiDS, LSST, WFIRST, Euclid) will be able to measure the matter power spectrum at scales down to $1 - 10$ h/Mpc with a few percent accuracy. Markovic et al. (2011); Smith & Markovic (2011) argued that the next generation of lensing surveys can provide sensitivity, compatible with the existing Lyman- α bounds (Viel et al. 2006; Seljak et al. 2006; Boyarsky et al. 2009a)). As in the case of the Lyman- α forest method the main challenge for the weak lensing is to properly take into account baryonic effects on matter power spectrum. The suppression of power spectrum due to primordial dark matter velocities can be extremely challenging to disentangle from the modification of the matter power spectrum due to baryonic feedback (Semboloni et al. 2011; van Daalen et al. 2011). Finally, the modified concentration mass relation can be probed with the weak lensing surveys (see e.g. Mandelbaum et al. 2008; King & Mead 2011) if their sensitivity can be pushed to halo masses below roughly $10^{12} M_{\odot}$.

While the observational difference between pure cold and mixed cosmologies is not drastic, clarifying this issue would have profound impact on the fundamental physics questions. Cold+Warm dark matter models are still in an infant state and an effort comparable with that, invested in theoretical investigation of structure formation of pure CDM may be needed before this question will be finally settled.

ACKNOWLEDGMENTS

We thank the anonymous referee whose comments have strongly improved the presentation of this paper. All numerical simulations were performed on the Theo and on

PanStarrs2 clusters of the Max-Planck-Institut für Astronomie at the Rechenzentrum in Garching.

REFERENCES

- Allgood B., Flores R. A., Primack J. R., Kravtsov A. V., Wechsler R. H., Faltenbacher A., Bullock J. S., 2006, *MNRAS*, 367, 1781
- Amorisco N. C., Evans N. W., 2011, *MNRAS*, 419, 184
- Asaka T., Shaposhnikov M., 2005, *Phys. Lett. B*, 620, 17
- Benson A. J., Frenk C. S., Lacey C. G., Baugh C. M., Cole S., 2002, *MNRAS*, 333, 177
- Bode P., Ostriker J. P., Turok N., 2001, *ApJ*, 556, 93
- Boyarisky A., Lesgourgues J., Ruchayskiy O., Viel M., 2009a, *JCAP*, 0905, 012
- Boyarisky A., Lesgourgues J., Ruchayskiy O., Viel M., 2009b, *Phys. Rev. Lett.*, 102, 201304
- Boyarisky A., Ruchayskiy O., Shaposhnikov M., 2009c, *Ann. Rev. Nucl. Part. Sci.*, 59, 191
- Boylan-Kolchin M., Bullock J. S., Kaplinghat M., 2011, *MNRAS*, 415, L40
- Bullock J. S., Kravtsov A. V., Weinberg D. H., 2000, *ApJ*, 539, 517
- Colin P., Avila-Reese V., Valenzuela O., 2000, *Astrophys. J.*, 542, 622
- Colin P., Valenzuela O., Avila-Reese V., 2008, *Astrophys. J.*, 673, 203
- Comerford J. M., Natarajan P., 2007, *Mon. Not. Roy. Astron. Soc.*, 379, 190
- Davis M., Efstathiou G., Frenk C. S., White S. D., 1985, *Astrophys. J.*, 292, 371
- de Naray R. K., Martinez G. D., Bullock J. S., Kaplinghat M., 2009
- Dodelson S., Widrow L. M., 1994, *Phys. Rev. Lett.*, 72, 17
- Dolgov A. D., Hansen S. H., 2002, *Astropart. Phys.*, 16, 339
- Dunstan R. M., Abazajian K. N., Polisensky E., Ricotti M., 2011
- Eke V. R., Navarro J., Steinmetz M., 2001, *Astrophys. J.*, 554, 114
- Feng J. L., 2010, *ARA&A*, 48, 495
- Hansen S. H., Lesgourgues J., Pastor S., Silk J., 2002, *MNRAS*, 333, 544
- Jing Y. P., Suto Y., 2002, *ApJ*, 574, 538
- King L. J., Mead J. M. G., 2011, *MNRAS*, 416, 2539
- Klypin A., Kravtsov A. V., Valenzuela O., Prada F., 1999, *ApJ*, 522, 82
- Klypin A. A., Trujillo-Gomez S., Primack J., 2011, *ApJ*, 740, 102
- Komatsu E., et al., 2009, *Astrophys. J. Suppl.*, 180, 330
- Lesgourgues J., Tram T., 2011, *JCAP*, 1109, 032
- Lewis A., Challinor A., Lasenby A., 2000, *Astrophys. J.*, 538, 473
- Lovell M. et al., 2012, *MNRAS*, 420, 2318
- Macciò A. V., Dutton A. A., van den Bosch F. C., 2008, *MNRAS*, 391, 1940
- Macciò A. V., Dutton A. A., van den Bosch F. C., Moore B., Potter D., Stadel J., 2007, *MNRAS*, 378, 55
- Macciò A. V., Fontanot F., 2010, *MNRAS*, 404, L16
- Macciò A. V., Kang X., Fontanot F., Somerville R. S., Kopev S., Monaco P., 2010, *MNRAS*, 402, 1995
- Macciò A. V., Stinson G., Brook C. B., Wadsley J., Couchman H. M. P., Shen S., Gibson B. K., Quinn T., 2012a, *ApJ*, 744, L9
- Macciò A. V., Paduroiu S., Anderhalden D., Schneider A., Moore B., 2012b, *MNRAS*, 424, 1105
- Mainini R., Macciò A. V., Bonometto S. A., Klypin A., 2003, *ApJ*, 599, 24
- Mandelbaum R., Seljak U., Hirata C. M., 2008, *JCAP*, 0808, 006
- Markovic K., Bridle S., Slosar A., Weller J., 2011, *JCAP*, 1101, 022
- Moore B., et al., 1999, *Astrophys. J.*, 524, L19
- Muñoz-Cuartas J. C., Macciò A. V., Gottlober S., Dutton A. A., 2011, *MNRAS*, 411, 584
- Navarro J. F., Frenk C. S., White S. D. M., 1997, *ApJ*, 490, 493
- Oh S.-H., de Blok W. J. G., Walter F., Brinks E., Kennicutt R. C., 2008, *AJ*, 136, 2761
- Palazzo A., Cumberbatch D., Slosar A., Silk J., 2007, *Phys. Rev.*, D76, 103511
- Papastergis E., Martin A. M., Giovanelli R., Haynes M. P., 2011, *Astrophys. J.*, 739, 38
- Polisensky E., Ricotti M., 2011, *Phys. Rev.*, D83, 043506
- Pontzen A., Governato F., 2012, *MNRAS*, 412, 3464
- Salucci P., Burkert A., 2000, *ApJ*, 537, L9
- Schneider A., Smith R. E., Macciò A. V., Moore B., 2012, *MNRAS*, 424, 684
- Seljak U., Makarov A., McDonald P., Trac H., 2006, *Phys. Rev. Lett.*, 97, 191303
- Seljak U., Zaldarriaga M., 1996, *Astrophys. J.*, 469, 437
- Semoloni E., Hoekstra H., Schaye J., van Daalen M. P., McCarthy I. J., 2011, *MNRAS*, 417, 2020
- Smith R. E., Markovic K., 2011, *Phys. Rev.*, D84, 063507
- Somerville R. S., 2002, *ApJ*, 572, L23
- Song H., Lee J., 2009, *Astrophys. J.*, 703, L14
- Spano M., Marcelin M., Amram P., Carignan C., Epinat B., Hernandez O., 2008, *MNRAS*, 383, 297
- Strigari L. E., Frenk C. S., White S. D. M., 2010, *MNRAS*, 408, 2364
- Strigari L. E., et al., 2006, *ApJ*, 652, 306
- Taoso M., Bertone G., Masiero A., 2008, *JCAP*, 0803, 022
- Tikhonov A., Gottlober S., Yepes G., Hoffman Y., 2009
- van Daalen M. P., Schaye J., Booth C. M., Vecchia C. D., 2011, *Mon. Not. Roy. Astron. Soc.*, 415, 3649
- Viel M., Becker G. D., Bolton J. S., Haehnelt M. G., Rauch M., Sargent W. L. W., 2008, *Phys. Rev. Lett.*, 100, 041304
- Viel M., Lesgourgues J., Haehnelt M. G., Matarrese S., Riotto A., 2005, *Phys. Rev.*, D71, 063534
- Viel M., Lesgourgues J., Haehnelt M. G., Matarrese S., Riotto A., 2006, *Phys. Rev. Lett.*, 97, 071301
- Viel M., Markovic K., Baldi M., Weller J., 2011, *MNRAS*
- Walker M. G., Penarrubia J., 2011, *Astrophys. J.*, 742, 20
- Warren, M. S., Abazajian, K., Holz, D. E., & Teodoro, L. 2006, *ApJ*, 646, 881
- Wang J., White S. D. M., 2007, *MNRAS*, 380, 93
- Wechsler R. H., Bullock J. S., Primack J. R., Kravtsov A. V., Dekel A., 2002, *ApJ*, 568, 52
- Zavala J., Jing Y., Faltenbacher A., Yepes G., Hoffman Y., et al., 2009, *Astrophys. J.*, 700, 1779